3D Real-Time Millimeter-Wave Camera

Christian Zech, David Schneider*, Axel Tessmann, and Sébastien Chartier
Fraunhofer Institute for Applied Solid State Physics IAF
GERMANY
(*now with IBM Deutschland GmbH)

christian.zech@iaf.fraunhofer.de, axel.tessmann@iaf.fraunhofer.de, sebastien.chartier@iaf.fraunhofer.de

ABSTRACT

Classic radar systems with only one transmit and receive channel are increasingly reaching their limits in military applications: The objects to be detected (such as projectiles or miniature drones) are becoming smaller, more agile and faster. On the other hand, imaging radars for detecting smallest objects with a correspondingly small radar cross-section, which is particularly challenging, are gaining increasing interest.

By coherent combination of multiple transmit and receive channels it is possible to not only measure the distance but also the angle of arrival of objects. However, a three-dimensional detection (distance, azimuth, elevation) requires a two-dimensional arrangement of the channels in order to determine both solid angles. Until now, for high-resolution measurements, this demands a high number of channels.

A novel 94 GHz millimeter-wave camera with hybrid antenna architecture significantly reduces the amount of high frequency hardware required. The system concept is fully implemented and verified in the form of a mobile demonstrator capable of soft real-time 3-D processing. By combining radio frequency components operating in the W band (85–105 GHz) with the presented aperture, a 3-D resolution of less than 1.5° x 1.5° x 15 cm is demonstrated using only eight transmitters and eight receivers.

1.0 INTRODUCTION

In the past, the development of radar systems has been driven by a fundamental property: Bandwidth yields range resolution. Therefore, the operating frequencies of the radio frequency (RF) components have been evolved to even higher frequencies in order to generate higher bandwidth. A better range resolution means, that the system is able to separate and distinguish closely spaced targets. As a result, it is possible to resolve even thinner layers of material structures [1], or detect tiny displacements in challenging industrial environments [2]. Radar transceivers with a usable bandwidth in the order of 10–50 GHz and an output power level suitable for close- to mid-range applications are becoming more and more available [3] – [6].

At the same time, there are a growing number of applications that benefit from the capability to resolve targets in one or even two angular dimensions [7] – [9]. Using only one transmit and receive channel to determine the angular direction of a target, mechanical scanning or (inverse) synthetic aperture radar (SAR) are in disadvantage due to scanning speed and possible mechanical failure. Electronical scanning using phased and/or reconfigurable arrays require precise phase control of the RF paths, which is challenging in terms of design, control and calibration, especially at higher operating frequencies. This usually leaves techniques relying on the synthesis of multiple physical channels, such as multiple-input–multiple-output (MIMO) arrangements, the best remaining option. MIMO systems have been successfully built and deployed, ranging from only a few to several thousand individual transmitters and receivers [10], [11].

2.0 ANTENNA APERTURE DESIGN

In order to localize a target in both angular dimensions, a MIMO radar requires a two-dimensional distribution of the transmit (Tx) and receive (Rx) channels. This is exemplary shown in Figure 1(a) using 16 Tx (orange circles) as well as 16 Rx channels (blue squares), resulting in a virtual array of 256 elements.

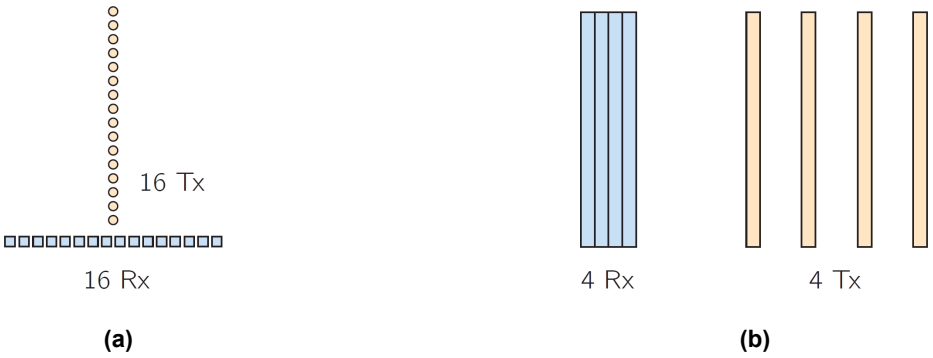

Figure 1: 2-D MIMO arrangement using 16 Tx (orange circles) and 16 Rx channels (blue squares) (a) and combination of frequency-scanning antennas with 1-D MIMO using only 4 Tx and 4 Rx channels (b). Both configurations can offer the same imaging capabilities.

Unfortunately, 2-D MIMO systems require a number of active channels that grows proportional to the targeted angular resolution. To double the angular resolution, twice the number of channels is required – in both dimensions. Depending on the requirements, this number can be reduced to some extent by trading angular resolution for sidelobe suppression in sparse and/or randomized arrangements [8], [10]. Nevertheless, a high channel count is especially undesirable when high-performance technologies, such as those based on III–V semiconductors, are involved due to their high per-channel cost and nontrivial medium-scale integration or when baseband processing power is limited due to power or portability constraints.

Modern semiconductor technologies allow very high operating bandwidths. If the available bandwidth of the hardware exceeds the application's requirement in terms of range resolution, an interesting trade-off becomes possible in the system design: Angular resolution can be increased at the cost of range resolution. This can be realised by exploiting frequency sensitive elements, usually antennas. The basic idea of this approach is to distribute the available bandwidth into multiple angular sectors without increasing the channel count.

Concepts based on the combination of frequency-sensitive elements with a linear MIMO aperture were already proposed by [12], [13]. The reported antenna structure, however, based on cost-effective technologies and comprising omnidirectional receivers and geometrically large, resonant slot transmitters, only allows for a moderate array directivity in the scanning plane as well as operating bandwidth and, correspondingly, combined angular/range resolution. The basic idea is shown in Figure 1(b) using four Tx as well as four Rx channels. This configuration has the same imaging capabilities as the one shown in Figure 1(a), with a dramatically reduced number of required channels.

For the presented system based on [14], we take up on the idea of combining frequency-steering antennas with 1-D MIMO but instead propose the integration of recently developed, highly directive leaky-wave antennas (LWAs) with fan beam characteristics [15] in the Tx and Rx paths of a linear MIMO array. As a result, the effectiveness and, consequently, the practical relevance of the hybrid frequency-scanning approach are significantly increased.

3.0 SYSTEM SETUP

At the Fraunhofer Institute for Applied Solid State Physics IAF, a millimeter-wave multichannel radar with a hybrid antenna architecture around 94 GHz has been realized for the first time. Our in-house III/V-compound semiconductor transistor technology offers, for example, very high operating bandwidths. The overall bandwidth of the components of 20 GHz can be divided into several angular segments using LWAs, resulting in high angular as well as high range resolution. The LWAs offer a scanning range of about 20°. By using eight Tx and eight Rx channels operating in the W band in the targeted array configuration (see Figure 1(b)), a uniform angular resolution of at least 1.5° x 1.5° with a range resolution of 10 cm to 15 cm is achieved. For comparison, a classic 2-D MIMO array with a comparable angular resolution would require eight times as many active channels. This combined resolution allows the discretization of the scene into voxels that are potentially more suitable for many mid-range imaging applications (e.g., 10–100 m) than approaches currently available.

3.1 RF Frontend

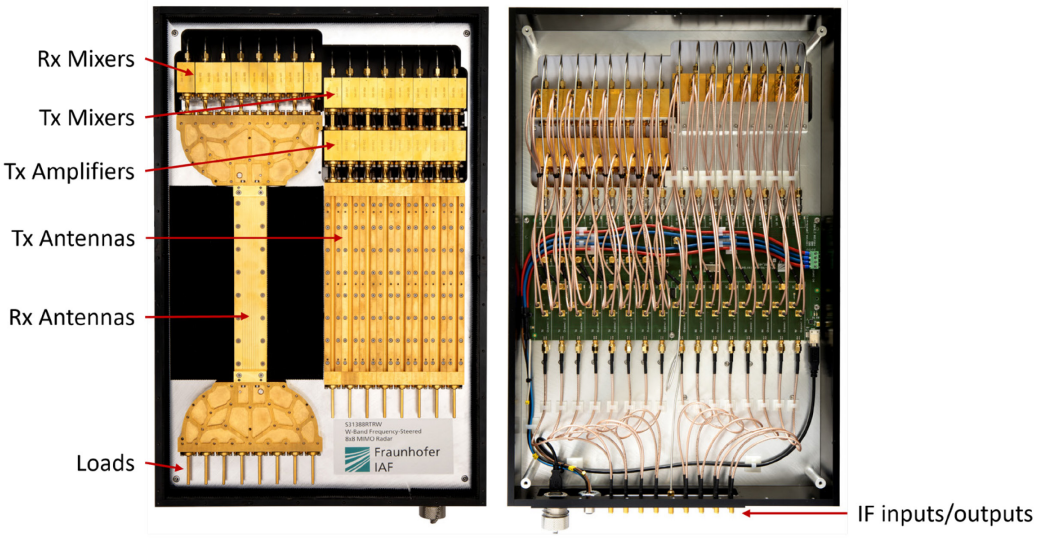

Figure 2: RF frontend from top side without radome (left) and backside (right).

The RF frontend consists of all high-frequency components and is shown in Figure 2. For the Tx path, an upconverting mixer with an additional medium power amplifier is used. The Rx comprises a low-noise amplifier with a downconverting mixer. A common local oscillator (LO) signal in the frequency range between 7 GHz and 9 GHz is distributed to all Tx and Rx channels and subsequently multiplied on-chip. The upconverter is realized as a double-balanced IQ mixer with an external 90° hybrid, resulting in single-sideband operation over an intermediate frequency (IF) range of approximately 90 MHz to 210 MHz. Similarly, the downconverter is based on a single-ended IQ mixer with the same external hybrid, thus operating as an image-reject mixer in the same frequency range.

All active components are fabricated as monolithic microwave integrated circuits (MMICs) on a 50 nm node of the Fraunhofer IAF InAlAs/InGaAs-based metamorphic high-electron-mobility transistor (mHEMT) technology and packaged in split-block modules with WR-10 waveguide flanges. The resulting combination of very low noise with a high operating bandwidth and output power is particularly beneficial to radar systems. Table 1 summarizes the typical active component specifications.

The realized antenna elements can be seen in the center of the left part of Figure 2. LO distribution and dc supply are integrated on the backside, as seen in the right part of the figure. The IF signals are routed via SMA cables from the mixer modules to the baseband unit.

Table 1: Typical RF component specifications.

Parameter		Value	Unit
Lower operating frequency		85	GHz
Upper operating frequency		105	GHz
Tx	Transmit channels	8	
	Conversion gain (singe sideband)	15	dB
	Saturated output power	15	dBm
	Output 1 dB compression point	11	dBm
	LO rejection	15	dB
	Sideband suppression	20	dB
Rx	Receive channels	8	
	Noise figure	3	dB
	Conversion gain	12	dB
	Image rejection	20	dB

3.2 Baseband Unit

The baseband unit mainly consists of the generation and digitalization of the IF signals for digital radar operation, as well as the LO generation. Due to the single-sideband or image-reject operation of the frontends, it features eight digital-to-analog converters (DACs) for the Tx channels and eight analog-to-digital converters (ADCs) for the Rx channels. The LO generation is based on a phase-locked loop (PLL) in combination with a wideband voltage-controlled oscillator (VCO).

3.3 Demonstrator

The 94 GHz millimeter-wave radar camera realized by Fraunhofer IAF is built in a standard 19” mobile rack to facilitate field testing, as seen in Figure 3. The RF frontend is mounted on top of the rack. The rack itself contains a standard personal computer with additional custom baseband processing hardware. It runs the analysis and control software that does most of the high-level processing, visualization, and user interfacing.

Figure 3: Photograph of the realized demonstrator in a mobile rack. On the top, the RF frontend and the user interface can be seen.

To demonstrate the system integration of the proposed frontend, we implement a multichannel stepped-carrier orthogonal frequency-division multiplexing (SC-OFDM) modulation scheme. OFDM radar is widely considered to be a promising technology for many spectrally dense scenarios requiring higher flexibility than conventional analog modulation [16].

4.0 MEASUREMENTS

4.1 Parking Deck

A measurement of nine trihedral reflectors mounted on plastic posts, each distributed at the same distance of 13 m but in different angular sectors, shows how clearly the millimeter-wave radar camera detects targets and distinguishes them from each other (Figure 4, drawn triangles represent real positions). As seen in the photograph, the measurement has been performed on a parking desk in order to avoid unwanted reflections. The RF frontend is located approximately 1.7 m above the ground. The angular resolutions in both dimensions do not differ qualitatively in spite of the different basic mechanisms (frequency steerable antennas / MIMO). This illustrates the cross-range imaging capabilities of the hybrid aperture concept.

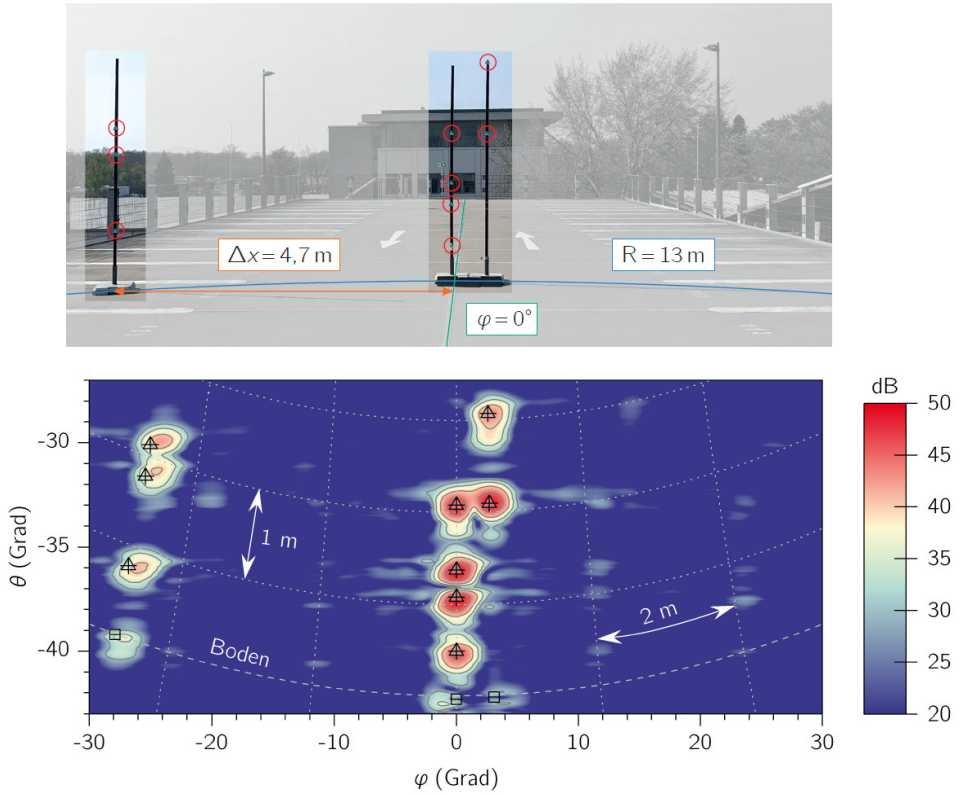

Figure 4: Photograph (top) and measurement (bottom) of an arrangement of trihedral reflectors illustrating the cross-range imaging performance of the system.

In Figure 5, the same but empty rectangular parking deck with a size of 18 m x 45 m featuring an enclosing metal fence is used as a test scene that primarily extends in range and azimuth direction. An elevation cut parallel to the ground is depicted in the bottom part of the figure, resolving a number of metal posts as well as the staircase behind the left part of the rear fence. The building in the center of the photograph also generates a distinct reflection at a range of 70 m, not shown in the radar image.

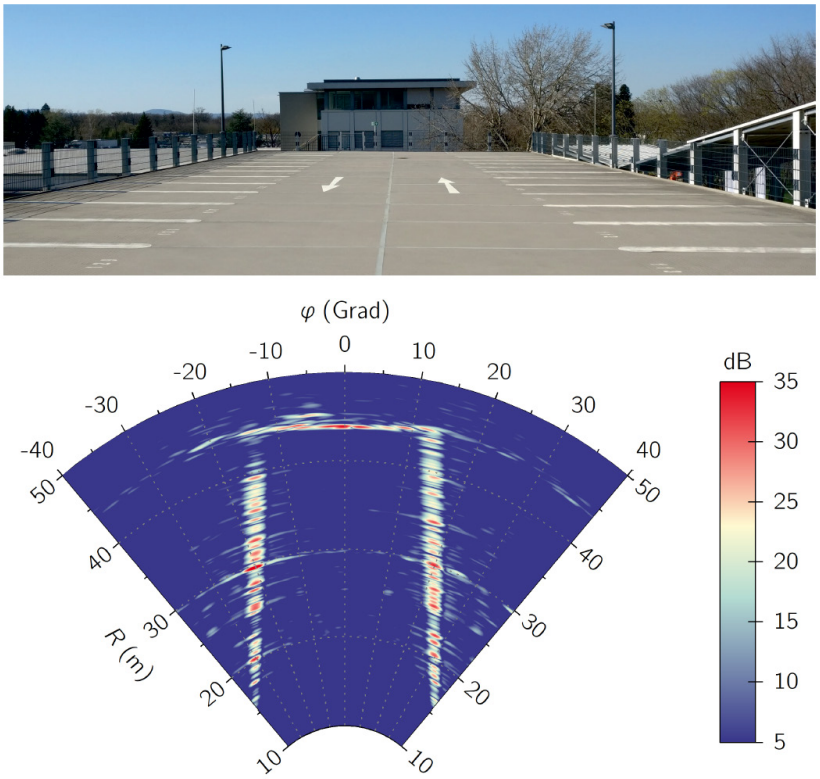

Figure 5: Photograph (top) and elevation cut of a radar image (bottom) showing a parking deck with a metal fence. Several individual posts of the fence are resolved as individual reflectors.

The same parking deck is shown in Figure 6 as 3-D plot. Here, an additional target in a range of 13 m is added that extends along the elevation direction (see inset). It consists of a post with 12 trihedral reflectors, mounted in equidistant steps of 35 cm. The RF frontend is in the origin of the coordinate system.

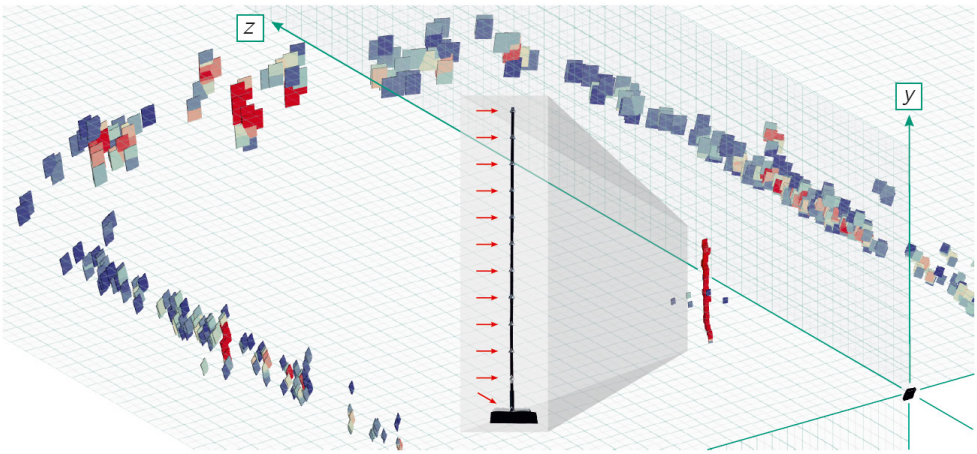

Figure 6: 3-D target plot of the parking desk with an additional vertical pole.

4.2 Miniature Drone

Another test has shown that the millimeter-wave camera of Fraunhofer IAF also succeeds in detecting small and moving targets with a correspondingly small radar cross-section, which is a particular challenge for imaging radars. On the radar image of a commercial miniature drone (DJI Mavic Pro 2, size approximately 33 cm x 25 cm x 9 cm) at a flight altitude of 10 m and a distance of about 32 m from the radar, the drone is clearly visible from the side (left part of the figure) as well as from the front (right part of the figure).

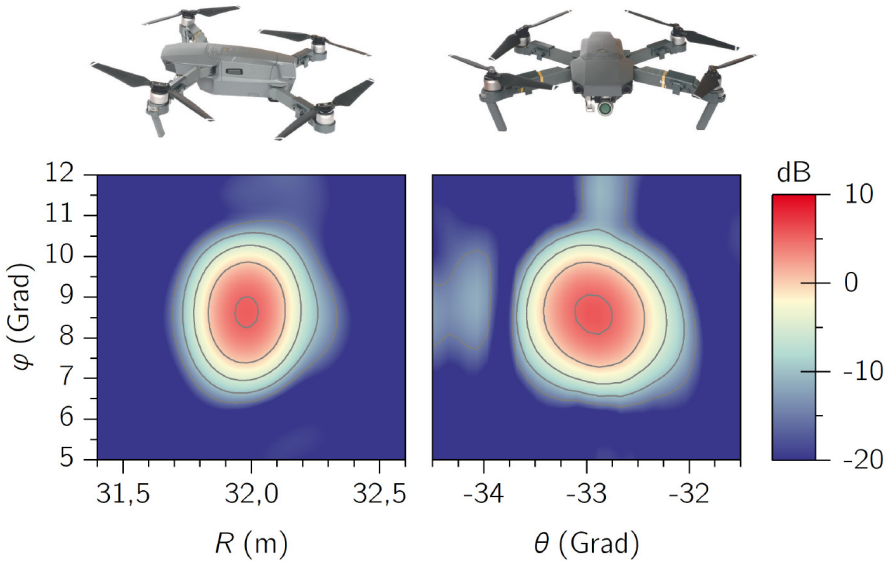

Figure 7: Cuts of the radar image of a small commercial drone (pictures not to scale).

5.0 CONCLUSION

A demonstrator featuring a hybrid antenna architecture combining frequency-steerable leaky-wave antennas with 1-D MIMO has been presented, in order to reduce the amount of required cost-intensive active channel count. The demonstrator operates in W band around 94 GHz and features a uniform angular resolution of at least 1.5° x 1.5° and a range resolution of at least 15 cm. Therefore, only eight Tx and eight Rx channels are used. A classic 2-D MIMO array would require eight times as many active channels.

Depending on the parameterization, the system is capable of achieving a frame rate of 5–25 frames per second. The demonstrator is thus suitable for mobile real-time imaging. A future application is conceivable, for example, for the high-resolution detection of projectiles or drones at close to medium range, as a 3-D landing aid under difficult visibility conditions, or for the protection of field camps.

6.0 REFERENCES

[1] D. Meier et al., “Propagation of millimeter waves in composite materials,” IEEE Trans. Antennas Propag., vol. 68, no. 4, pp. 3080–3093, Apr. 2020.

[2] T. Jaeschke, C. Bredendiek, and N. Pohl, “A 240 GHz ultra-wideband FMCW radar system with on-chip antennas for high resolution radar imaging,” in IEEE MTT-S Int. Microw. Symp. Dig., Jun. 2013, pp. 1–4.

[3] C. Zech et al., “A compact W-band LFMCW radar module with high accuracy and integrated signal processing,” 2015 European Microwave Conference (EuMC), Paris, France, 2015, pp. 554-557, doi: 10.1109/EuMC.2015.7345823.

[4] N. Pohl, T. Jaeschke, and K. Aufinger, “An ultra-wideband 80 GHz FMCW radar system using a SiGe bipolar transceiver chip stabilized by a fractional-N PLL synthesizer,” IEEE Trans. Microw. Theory Techn., vol. 60, no. 3, pp. 757–765, Mar. 2012.

[5] S. Yuan, A. Trasser, and H. Schumacher, “56 GHz bandwidth FMCW radar sensor with on-chip antennas in SiGe BiCMOS,” in IEEE MTT-S Int. Microw. Symp. Dig., Jun. 2014, pp. 1–4.

[6] T. Spreng, S. Yuan, V. Valenta, H. Schumacher, U. Siart, and V. Ziegler, “Wideband 120 GHz to 140 GHz MIMO radar: System design and imaging results,” in Proc. Eur. Microw. Conf. (EuMC), Sep. 2015, pp. 430–433.

[7] H. Wilden, J. Klare, A. Froehlich, and M. Krist, “MIRACLE, an experimental MIMO radar in Ka band,” in Proc. Eur. Conf. Synth. Apert. Radar (EUSAR), Jun. 2010, pp. 382–385.

[8] D. Bleh et al., “W-band time-domain multiplexing FMCW MIMO radar for far-field 3-D imaging,” IEEE Trans. Microw. Theory Techn., vol. 65, no. 9, pp. 3474–3484, Sep. 2017.

[9] W. Johannes, M. Caris, and S. Stanko, “94 GHz radar used for perimeter surveillance with wide target clarification,” in Proc. 21st Int. Radar Symp. (IRS), Oct. 2020, pp. 15–18.

[10] R. Feger, C. Wagner, S. Schuster, S. Scheiblhofer, H. Jager, and A. Stelzer, “A 77-GHz FMCW MIMO radar based on an SiGe single-chip transceiver,” IEEE Trans. Microw. Theory Techn., vol. 57, no. 5, pp. 1020–1035, May 2009.

[11] S. S. Ahmed, A. Schiessl, and L.-P. Schmidt, “A novel fully electronic active real-time imager based on a planar multistatic sparse array,” IEEE Trans. Microw. Theory Techn., vol. 59, no. 12, pp. 3567–3576, Dec. 2011.

[12] A. Orth, P. Kwiatkowski, and N. Pohl, “A novel approach for a MIMO FMCW radar system with frequency steered antennas for 3D target localization,” in Proc. Eur. Radar Conf. (EuRAD), Oct. 2019, pp. 37–40.

[13] A. Shoykhetbrod, H. Cetinkaya, and S. Nowok, “Measurement-based performance investigation of a hybrid MIMO-frequency scanning radar,” in IEEE MTT-S Int. Microw. Symp. Dig., Aug. 2020, pp. 1251–1254.

[14] D. A. Schneider, M. Rösch, A. Tessmann und T. Zwick. „Hybrid Beam-Steering OFDM-MIMO Radar: High 3-D Resolution With Reduced Channel Count”. In: IEEE Transactions on Microwave Theory and Techniques 69.11 (2021), S. 5057–5071. DOI: 10.1109/TMTT.2021.3104296.

[15] D. A. Schneider, M. Rösch, A. Tessmann and T. Zwick, “A Low-Loss W-Band Frequency-Scanning Antenna for Wideband Multichannel Radar Applications,” in IEEE Antennas and Wireless Propagation Letters, vol. 18, no. 4, pp. 806-810, April 2019, doi: 10.1109/LAWP.2019.2904170.

[16] G. Hakobyan and B. Yang, “High-performance automotive radar: A review of signal processing algorithms and modulation schemes,” IEEE Signal Process. Mag., vol. 36, no. 5, pp. 32–44, Sep. 2019.